The impact of satellite altimetry data on the NCEP Global Ocean Data Assimilation System

David W. Behringer
NOAA/NCEP Environmental Modeling Center, 5200 Auth Rd. W/NP23, Camp Springs MD, 20746, USA
July 26, 2005

1 Introduction

For over 10 years the National Centers for Environmental Prediction (NCEP) has employed coupled ocean-atmosphere numerical models for making seasonal to interannual climate forecasts in an operational or quasi-operational mode (Ji et al., 1995; Ji et al., 1998; Saha et al., 2005). A critical element of the forecast effort is an ocean data assimilation system (ODAS) that provides an estimate of the ocean state to initialize the coupled forecasts. The original ODAS was based on the Geophysical Fluid Dynamics Laboratory (GFDL) Modular Ocean Model version 1 (MOM.v1) and was configured for the Pacific Ocean (Ji et al., 1995). The data assimilation method was a three-dimensional variational (3DVAR) scheme devised by Derber and Rosati (1989). The Pacific ODAS was later modified to incorporate revised background error covariances (Behringer et al. 1998) and to assimilate satellite altimetry data (Vossepoel and Behringer, 2000; Ji et al., 2000).

Over the last few years a new global ocean data assimilation system (GODAS) was developed to be the replacement for the Pacific ODAS, and to provide the oceanic initial conditions for the new NCEP coupled Climate Forecast System (CFS). The GODAS became operational in 2003 and the CFS went operational in 2004. A simple description of the GODAS is provided by Behringer and Xue (2004), and a more detailed paper is in preparation. The purpose of this report is to describe the impact of the addition of satellite altimetry data to the standard or operational GODAS. The report begins with a short description of the standard GODAS, continues with a description of the altimetry data and how they are assimilated and concludes with a results section comparing the altimetry assimilation experiment with a Control that assimilates no data and with the standard GODAS.

2 The Standard Operational GODAS

The GODAS is based on a quasi-global configuration of the GFDL MOMv3 (Pacanowski and Griffies, 1998). The model domain extends from 75^{O}S to 65^{O}N and has a resolution of 1^{O} by 1^{O} enhanced to $1/3^{O}$ in the N-S direction within 10^{O} of the equator. The model has 40 levels with a 10 meter resolution in the upper 200 meters. This configuration represents a small improvement over the Pacific ODAS which had a 1.5^{O} resolution in the E-W direction and 28 levels in the vertical. Other new features include an explicit free surface, the Gent-McWilliams isoneutral mixing scheme and the KPP vertical mixing scheme. The GODAS is forced by the momentum flux, heat flux and fresh water flux from the NCEP atmospheric Reanalysis 2 (R2) (Kanamitsu et al. 2002). In addition the temperature the top model level is relaxed to weekly analyses of sea surface temperature (Reynolds et al., 2002), while the surface salinity is relaxed to annual salinity climatology (Conkright et al., 1999). Very short relaxation periods are used (5 days for temperature and 10 days for salinity). The GODAS assimilates temperature profiles and, in another new feature, assimilates synthetic salinity profiles as well. The assimilation method is the same 3DVAR scheme used in the Pacific ODAS, but it has been modified to assimilate salinity and the code has been rewritten to run in a multi-processor computing environment.

The standard GODAS has been used for a long reanalysis extending from 1979 to the present. In this reanalysis GODAS assimilates temperature profiles from XBTs, from TAO, TRITON and PIRATA moorings (McPhaden et al., 2001) and from Argo profiling floats (The Argo Science Team, 2001). The XBT observations collected prior to 1990 were acquired from the NODC World Ocean Database 1998 (Conkright et al., 1999), while the XBTs collected subsequent to 1990 are acquired from the Global Temperature-Salinity Profile Project. A synthetic salinity profile is computed for each temperature profile using a local T-S climatology based on the annual mean fields of temperature and salinity from the NODC World Ocean Database (Conkright et al., 1999). Figure 1 shows the monthly counts of the temperature profiles used in GODAS. The number of profiles can vary significantly from month to month, but there are longer term trends as well. For example, there is a gradual decline in the monthly counts after 1985 followed by a sharp recovery in 1990 when the source of the profiles changed.

There are also changes in the distribution of the profiles. For example, the TAO moorings represent a fixed array of daily observations in the tropical Pacific Ocean that has no counterpart in the 1980s. More recently the rapid growth of the Argo network represents both an important increase in the number of profiles and a departure from the older XBT network for which the profiles are confined to ship tracks. Figure 2 gives some flavor of the changes in the geographical distribution of the profiles, most notably the expansion of the Argo array between 2002 and 2004 and the improvement in coverage of the southern hemisphere during this time. All of these changes in the data suite will have an impact on the GODAS analysis. However, for this report we are only concerned with the period of satellite altimetry beginning in 1993 and extending through the present. While during this period the overall observational suite experiences important changes, the Tao array remains relatively constant and the abrupt discontinuity in 1990 in the XBT distribution is avoided.

3 The assimilation of satellite altimetry data

The standard GODAS 3DVAR scheme is essentially the same as the original Derber and Rosati (1989) scheme, although it has been adapted to assimilate salinity in addition to temperature. In order to assimilate sea surface height (SSH) observations further modifications are necessary. These same modifications were made earlier to the Pacific ODAS and are described in Behringer et al. (1998) and Ji et al. (2000), but will be covered briefly here as well. The modified 3DVAR scheme minimizes a functional,

$$\mathbf{I} = \tfrac{1}{2}\{\mathbf{T}^{\mathrm{T}}\mathbf{E}^{-1}\mathbf{T}\} + \tfrac{1}{2}\{[D(\mathbf{T}) - \mathbf{T}_0]^{\mathrm{T}}\mathbf{F}^{-1}[D(\mathbf{T}) - \mathbf{T}_0] + [D(L\mathbf{T}) - \delta\mathbf{Z}_0]^{\mathrm{T}}\mathbf{G}^{-1}[D(L\mathbf{T}) - \delta\mathbf{Z}_0]\}$$

where the vector $\mathbf{T}$ represents the correction to the first-guess prognostic tracers (temperature and salinity) computed by the model, $\mathbf{E}$ is the first guess error covariance matrix, $\mathbf{T}_0$ represents the difference between the tracer observations and the first-guess, D is an interpolation operator that transforms the first-guess tracers from the model grid to the observation locations, $\mathbf{F}$ is the observation error covariance matrix for the tracers, L is a linear operator that transforms a vertical column of temperature and salinity corrections into an estimate of the correction to the first-guess dynamic height field, $\mathbf{G}$ is the observation error covariance matrix for SSH, and $\delta\mathbf{Z}_0$ represents the difference between the observed and first-guess SSH fields. The observational errors are assumed to be uncorrelated, so the matrices, $\mathbf{F}$ and $\mathbf{G}$, have only diagonal elements, which are the error variances of the observations. The last term on the right-hand side is a constraint imposed by the observed SSH. It would be pointless to correct the model SSH directly; instead, the SSH observations are used to impose an integral vertical constraint on the corrected model temperature and salinity fields. The relative magnitudes of these corrections throughout the water column depend on the vertical structure of the first-guess error covariance matrix. In other words, the

assimilation system preferentially corrects the model temperature and salinity where their expected errors are greatest, making those corrections in such a way as to bring the model surface dynamic height into closer agreement with the SSH observations. An implied assumption in this approach is that we can use the SSH observations to correct only the baroclinic part of the model SSH and that it is safe to neglect the barotropic part. In the Tropics, our main region of interest, this may be a reasonable assumption.

The 3DVAR scheme avoids the problem of knowing the absolute SSH by assimilating only the variable part of the SSH and so in the minimization of the cost function the altimetry data and first-guess model SSH data each have their own long-term mean removed. In the case of the model data a 1993–99 seven-year mean is computed from the output of the standard GODAS reanalysis.

Two experiments have been done that assimilate satellite altimetry. The first of these assimilates a merged TOPEX and Jason-1 dataset and runs from 1993 through 2003 while the second assimilates a merged ERS-2 and Envisat dataset and runs from 1996 through 2003. In these experiments only the data between 30^{o}S and 40^{o}N were assimilated. The data sets were provided by the AVISO SSALTO/DUACS as two internally consistent time series of sea surface height deviations, relative to a 1993–99 seven-year mean. Both data sets were processed to remove residual orbit error, and to ensure compatibility between missions. The TOPEX/Jason data were corrected based on internal crossovers, while the ERS/Envisat data were adjusted to the TOPEX/Jason data to eliminate residual orbit error (Le Traon and Ogor, 1998; Lillibridge et al., 2005). Figure 3 shows two examples of the along-track data at the time of the 1997-98 El Nino as they are assimilated into the GODAS. The 10-day TOPEX cycle (12/28/97-1/7/98) and the 35-day ERS-2 cycle (12/14/97-1/18/98) overlap in time and illustrate the excellent degree of compatibility between the data sets. Table 1 lists information about the satellite missions.

4 Evaluation

In this section the results of the altimetry assimilation experiments are compared to the satellite altimetry data itself, island tide gauge data, Argo temperature and salinity profiles and zonal current profiles from the TAO array. To evaluate the impact of the altimetry data on the GODAS, the same comparisons will be made using the results from the standard GODAS reanalysis and from a Control run of the ocean model that is forced by the same R2 data but that does not assimilate any observations. Table 2 summarizes the model experiments.

4.1 Comparisons with satellite altimetry

For the purpose of these comparisons a simple OI scheme was used to make monthly maps of the TOPEX/Jason satellite altimetry on the GODAS grid. The maps represent monthly deviations of SSH from the 1993-99 mean. In the comparisons that follow each field has also had its own mean monthly climatology removed so that only the anomaly fields are compared. The maps were compared to the monthly average SSH anomalies from the Control, the standard GODAS analysis and the GODAS analysis that assimilates the TOPEX/Jason data. Figure 4 shows the correlations and RMS differences between the observations and the model results for the period 1993-2003. In the top two panels it can be seen that the Control does a reasonable job in the equatorial Pacific and Indian Oceans. Once outside the equatorial zone the correlations drop off and the RMS differences in the central and western North Pacific and western South Pacific can become as large as 8 cm. The Control does a poor job of simulating the SSH in the Atlantic Ocean. Correlations are low everywhere and negative in the subtropics. In the middle panels, the standard GODAS, assimilating temperature and synthetic salinity, shows the impact of

the TAO array in the Pacific where the band of correlations greater than 0.8 has become broader compared to the Control and the large RMS differences in the western Pacific have been greatly reduced. The standard GODAS shows improvement over the Control in the Atlantic Ocean as well. The negative SSH correlations in the North Atlantic are gone although not in the South Atlantic and elsewhere the correlations are stronger although not to the same extent as in the Pacific. In the Indian Ocean the standard GODAS shows no improvement over the Control. The patterns in the correlation and RMS difference fields in the Indian Ocean are similar for the Control and the standard GODAS, suggesting that what skill exists there comes from the model itself. This is a reflection of the relatively poorer distribution of assimilation data in the Indian Ocean as compared with the Pacific and Atlantic Oceans. Finally, in the bottom panels the GODAS analysis that assimilates the satellite SSH data is compared with that same data. It is therefore not an independent test of the analysis. Nevertheless, the assimilation of the SSH data has resulted in broad improvements in the model SSH. Correlations are 0.8 or better almost everywhere. In the Indian Ocean, where the standard GODAS SSH did not improve on the Control, correlations are higher and RMS differences are generally lower. In the Atlantic, the SSH correlations with the observations are everywhere comparable to those in the Pacific, while in the standard GODAS they had been relatively weak. The RMS differences of model SSH with observations are less than 3 cm over large portions of the Atlantic and Pacific. In the tropics the RMS differences remain somewhat larger (4-5 cm) in the region of the tropical instability waves and the recirculation of the Brazil current.

Similar comparisons were made to monthly maps based on the ERS-2/Envisat SSH anomalies. In this case a GODAS analysis that assimilated the ERS-2/Envisat data was used in the comparisons along with the Control and the standard GODAS. The results are shown in Figure 5. The comparisons are nearly identical with those for the TOPEX/Jason SSH data shown in Figure 4. Some slight differences do occur, but they may simply be due to the shorter time span of the ERS-2/Envisat experiment (1996-2003) than for the TOPEX/Jason experiment (1993-2003). It is encouraging find that, on monthly time-scales, the ERS-2/Envisat missions could provide the capability for the assimilation of altimetric SSH data if residual orbit errors can be properly removed.

4.2 Comparisons with island tide gauges

We next compare the model output with island tide gauge data. The tide gauge data are not assimilated and are thus independent of all the model runs. Research quality tide gauge data were acquired from the University of Hawaii Sea Level Center in the form of monthly average SSHs. Information about the gauges used here is listed in Table 3. The comparisons are confined to the tropics, six in the Pacific Ocean and one in the Atlantic Ocean. The time-series are shown in Figure 6 for the tide gauge SSHs and the model SSHs interpolated to the gauge locations. Each time-series has its own mean removed. The RMS differences and correlations for each tide gauge / model pair are listed in Table 4. The gauges shown in Figure 6a are near or outside the margins of the TAO array in the western Pacific. The Control captures the large events, but it also has large departures from the tide gauge records, most noticeably at Guam. The assimilation of temperature and salinity largely corrects the standard GODAS analysis and the assimilation of altimetry SSH data corrects the GODAS analyses even further. For these latter analyses the RMS errors are 2-3 cm and the correlations with the tide gauge SSH exceed 0.9 (Table 4). Figure 6b shows three gauges that are within one degree of the equator, two in the western Pacific and one in the Galapagos in the eastern Pacific. For this group the SSH in the Control is closer to the SSH in the three GODAS analyses, even capturing the double peak of the 1997 El Nino and some of the subsequent small variations at the Galapagos. In the western Pacific none of the model runs capture the extreme amplitudes of the 1997 event. They also miss several questionable small

spikes in the 2001-02 tide gauge records at the two western sites. At the Galapagos site all three GODAS analyses perform very well; the RMS errors are 2-3 cm and the correlations exceed 0.96 (Table 4). At Limetree Bay in the Atlantic basin the standard deviation of the tide gauge time-series is about half the magnitude of the standard deviations at the Pacific sites and the correlations between the tide gauge SSHs and the model SSHs are lower here than at the Pacific sites (Table 4). Nevertheless, the model runs do capture the three large oscillations in the tide gauge record between 1993 and 2001 (Figure 6c).

4.3 Comparisons with observed temperature and salinity profiles

The next comparisons are between the model analyses and observed temperature profiles from the Argo floats and from the TAO and PIRATA moorings for the years 2000-2004. All of the GODAS analyses assimilate these observations so they are only independent of the Control. The difference between a model analysis and an observed profile is formed by interpolating the 5-day model output to the time and position of the observation and subtracting the observed from the model profile. Figure 7 shows the profiles of the mean and RMS differences for 5 latitude bands: 65^{o}S-30^{o}S, 30^{o}S-10^{o}S, 10^{o}S-10^{o}N, 10^{o}N-30^{o}N and 30^{o}N-65^{o}N. The upper panel in Figure 7a shows the comparisons for the Control; the largest mean errors are 1-2^{o}C and the largest RMS errors are 2-3^{o}C. The comparisons for the standard GODAS analysis are shown in the lower panel of Figure 7a. By assimilating these temperature data the mean differences are reduced to less than 0.06^{o}C and the RMS differences are reduced to less than 1.5^{o}C. In the tropics and subtropics the RMS differences drop off to less than 0.5^{o}C below 100 meters. The two panels in Figure 7b show the nearly identical comparisons for the TOPEX/Jason-1 and ERS-2/Envisat GODAS analyses. The altimetry data was only assimilated between 30^{o}S and 40^{o}N so the comparisons for the southernmost and northernmost bands are essentially unchanged from those for the standard GODAS. In the tropics and subtropics the temperature differences between the model and the observations above 400 meters are nearly the same for the altimetry analyses as for the standard GODAS analysis. However, below 400 meters the mean temperature differences for the altimetry analyses increase with depth to 0.25-0.5^{o}C. Thus in these experiments the assimilation of altimetry improves the representation of SSH variability in GODAS while degrading slightly the temperature field below 400 meters. We will return to this point later in the discussion section.

Similar comparisons were done between the model analyses and observed salinity profiles from the Argo floats. All of these GODAS experiments assimilate only synthetic salinity profiles so the observed salinity profiles are independent of all the model analyses. Figure 8 shows the comparisons for the same latitude bands as for the temperature comparisons in Figure 7. The upper panel in Figure 8a shows the comparisons for the Control. At the surface the mean errors range between -0.1and 0.2 psu while the RMS errors range between 0.4 and 1.0 psu. The comparisons for the standard GODAS analysis are shown in the lower panel of Figure 8a. It is clear that the assimilation of synthetic salinity greatly reduces the mean error in the salinity field and reduces the RMS error by about 50%. The largest errors in both the Control and the standard GODAS are in the northern subtropics. Figure 8b shows the salinity comparisons for the TOPEX/Jason-1 and ERS-2/Envisat GODAS analyses. As with the temperature comparisons the salinity comparisons for the southernmost and northernmost bands are essentially unchanged from those for the standard GODAS. Also, as with the temperature comparisons, there is a slight degradation in the comparison with the observed salinity profiles when the altimetry is assimilated; this effect is largest in the northern subtropics.

4.4 Comparison with current observations

A final set of comparisons was made between the model results and the zonal currents observed at five TAO locations along the equator in the Pacific Ocean. Table 5 lists their positions and the time periods for which data are available. Zonal currents from the model analyses were interpolated to the same times and locations as the observations. The means and standard deviations for all of these time series are shown in Figure 9. In the top panel the mean zonal currents in the three GODAS analyses are nearly identical; the assimilation of the altimetry data has had little effect beyond what has already been achieved by the assimilation of temperature and salinity. East of the dateline all of the model analyses get the depth of the undercurrent core reasonably correct. The magnitude of the undercurrent in the GODAS analyses is good at 170^{o}W and 140^{o}W, but it is too weak at 110^{o}W; the undercurrent in the Control is too weak at all three locations. In the GODAS analyses the eastward flow beneath the undercurrent core at 110^{o}W and below 200 m elsewhere is too strong and the westward surface flow at 170^{o}W and 140^{o}W is too weak. The Control run displays none of these deficiencies, suggesting that they may be artifacts of the assimilation process. West of the dateline, at 147^{o}E all of the model currents have an eastward bias over most of profile depth and they fail to capture the change in direction seen in the observations at 150 m. At 165^{o}E the undercurrent core in all of the model runs is too shallow and too broad. Also at 165^{o}E the currents in the GODAS analyses are too strong to the east between 50 and 150 m and too strong to the west above 50 m, while the currents in the Control run are reasonably good in these layers.

The lower panel in Figure 9 shows profiles of the standard deviation of the zonal flow at the five locations. If we discount the additional structure in the observed standard deviations in the upper layers, the general agreement between the model and observed currents is good. The currents in the GODAS experiments that assimilate altimetry data show more variability below 150 m at the three western locations and the currents in all the model experiments show this behavior at the westernmost site at 147^{o}E.

5 Discussion

It is clear from these experiments that the addition of altimetry data sets to the standard operational GODAS leads to broad improvements in the representation of SSH in the analysis. However, as has been noted in the foregoing presentation the improvement in SSH has been accompanied by some loss of accuracy elsewhere. For example, assimilating altimetry has led to an increase in the RMS error in temperature and salinity below 400 m in the northern subtropics and an increase in the variability of the zonal currents below 150 m in the western equatorial Pacific. There are also pre-existing problems in the standard GODAS that have not been improved by the assimilation of altimetry. For example, the undercurrent at 110^{o}W remains too diffuse and too weak, while the surface currents maintain an eastward bias at 170^{o}W and 140^{o}W and a westward bias at 14^{o}7E and 165^{o}E.

Some of these difficulties may be related to the fundamental problem of model bias that is common to all of these experiments. If we can succeed in reducing model bias through improvements to the model physics and to the forcing fields, we can expect the assimilation system to perform better regardless of the combinations of data that are assimilated.

Other simple technical improvements to the assimilation system may have a positive effect as well and these will be explored in the near future. The first of these is to extend the depth over which the assimilation is performed. In the experiments described here the data assimilation extends only down to 750 m, the typical depth limit of most XBT probes. Pushing the lower limit to 1500-2000 m would make better use of the growing number of Argo profiles and allow a greater range for temperature and salinity adjustments required by the assimilation of

altimetry. A possible benefit to GODAS might be improved SSH without an increase in the RMS error in temperature and salinity below the thermocline. The second technical change would be to impose a partial geostrophic balance in the assimilation scheme. This has been shown to have a positive effect on the tropical and equatorial circulation (Burgers et al., 2002; Weaver et al., 2003) and may help to improve the surface equatorial currents in the western Pacific in GODAS. A final improvement would be to replace the synthetic salinity profiles that are used in the standard GODAS with observed Argo salinity profiles wherever they are available. Some work has already been done on this last project and the results will be the subject of another report similar to the present one.

Acknowledgements

The Argo data were collected and made freely available by the International Argo Project and the national programmes that contribute to it. (http://www.argo.ucsd.edu, http://argo.jcommops.org). Argo is a pilot programme of the Global Ocean Observing System.

The altimeter products were produced by Ssalto/Duacs as part of the Environment and Climate EU Enact project (EVK2-CT2001-00117) and distributed by Aviso, with support from Cnes

The tide gauge data were made available by the University of Hawaii Sea Level Center (http://uhslc.soest.hawaii.edu).

References

Argo Science Team, 2001: The global array of profiling floats. *Observing the Ocean in the 21st Century*. C. J. Koblinsky and N. R. Smith, Eds., Australian Bureau of Meteorology, 248–258.

Behringer, D.W., M. Ji, and A. Leetmaa, 1998: An improved coupled model for ENSO prediction and implications for ocean initialization. Part I: The ocean data assimilation system. *Mon. Wea. Rev*., **126**, 1013-1021.

Behringer, D.W., and Y. Xue, 2004: Evaluation of the global ocean data assimilation system at NCEP: The Pacific Ocean. *Eighth Symposium on Integrated Observing and Assimilation Systems for Atmosphere, Oceans, and Land Surface, AMS 84th Annual Meeting, Washington State Convention and Trade Center, Seattle, Washington, 11-15*.

Burgers, G., M. A. Balmaseda, F. C. Vossepoel, G. J. van Oldenborgh, and P. J. van Leeuwen, 2002: Balanced ocean data assimilation near the equator, J. Phys. Oceanogr., 32, 2509-2519.

Conkright, M.E., S. Levitus, T. O'Brien, T.P. Boyer, C. Stephens, D. Johnson, O. Baranova, J. Antonov, R. Gelfeld, J. Rochester, C. Forgy, 1999: World Ocean Database 1998, Documentation and Quality Control Version 2.0, National Oceanographic Data Center Internal Report 14, National Oceanographic Data Center, Silver Spring, MD.

Derber, J.C., and A. Rosati, 1989: A global oceanic data assimilation system. *J. Phys. Oceanogr*., **19**, 1333-1347.

Ji, M., A. Leetmaa, and J. Derber, 1995: An ocean analysis system for seasonal to interannual climate studies. *Mon. Wea. Rev*., **123**, 460-481.

Ji, M., R.W. Reynolds, and D.W. Behringer, 2000: Use of TOPEX/Poseidon sea level data for ocean analyses and ENSO prediction: Some early results. *J. Climate*, **13**, 216-231.

Ji, M. D.W. Behringer, and A. Leetmaa, 1998: An improved coupled model for ENSO prediction and implications for ocean initialization. Part II: The coupled model. *Mon. Wea.. Rev*., **126**, 1022-1034.

Kanamitsu, M., W. Ebisuzaki, J. Woolen, S.-K. Yang, J.J. Hnilo, M. Fiorino, and G.L. Potter, 2002: NCEP-DOE AMIP-II reanalysis (R-2). *Bull. Amer. Meteor. Soc*., **83**, 1631-1643.

Lillibridge, J., D. Behringer, Y. Xue and J. Kuhn, 2005: Improving ocean analyses and ENSO forecasts at NOAA using the global ocean data assimilation system and altimetric sea level

Le Traon, P.-Y., and F. Ogor, 1998: ERS-1/2 orbit improvement using TOPEX/Poseidon: the 2 cm challenge, J. Geophys. Res., 103 (C4), 8045-8057.

McPhaden, M. J., T. Delcroix, K. Hanawa, Y. Kuroda, G. Meyers, J. Picaut, and M. Swenson, 2001: The El Niño/Southern Oscillation (ENSO) Observing System. *Observing the*

Ocean in the 21st Century, C. J. Koblinsky and N. R. Smith, Eds., Australian Bureau of Meteorology, 231–246.

Pacanowski, R.C. and S. M. Griffies, 1998: MOM 3.0 Manual. NOAA /Geophysical Fluid Dynamics Laboratory, Princeton, NJ, USA 08542.

Reynolds, R. W., N. A. Rayner, T. M. Smith, D. C. Stokes and W. Wang, 2002: An improved in situ and satellite SST analysis for climate. J. Climate, **15**, 1609-1625.

Saha' S., S. Nadiga, C. Thiaw, J. Wang, W. Wang, Q. Zhang, H. M. van den Dool, H.-L. Pan, S. Moorthi, D. Behringer, D. Stokes, G. White, S. Lord, W. Ebisuzaki, P. Peng, P. Xie, 2005: The NCEP Climate Forecast System. *Submitted to J. Climate.*

Vossepoel, F. C. and D. W. Behringer, 2000: Impact of sea level assimilation on salinity variability in the western equatorial Pacific. J. Phys. Oceanogr., **30**, 1706-1721.

Weaver, A. T., J. Vialard, and D. L. T. Anderson, 2003: Three- and four-dimensional variational assimilation with a general circulation model of the tropical Pacific Ocean. Part I: Formulation, internal diagnostics, and consistency checks. Mon. Wea. Rev., **131**, 1360–1378.

Table 1. Satellite Mission Information			
Satellite	**Cycles**	**Start Date**	**End Date**
TOPEX	002-364	1992-10-02	2002-08-11
Jason-1	022-074	2002-08-11	2004-01-18
ERS-2	001-085	1995-05-16	2003-06-22
Envisat	017-023	2003-06-22	2004-02-03

Table 2. Description of model experiments			
Name	**Forcing**	**Assim Data**	**Status**
Control	Reanalysis 2	None	Developmental
GODAS - Standard	Reanalysis 2	Temperature, Salinity	Operational
GODAS – T / J	Reanalysis 2	Temp., Sal., Topex/Jason-1	Developmental
GODAS – E / J	Reanalysis 2	Temp., Sal., ERS-2/Envisat	Developmental

Table 3. Tide Gauge Information					
Sta	**Location**	**Country**	**Lat**	**Long**	**Years**
053	Guam	USA Trust	13-26N	144-39E	1948-2003
005	Majuro-B	Rep. Marshall I.	07-07N	171-22E	1993-2003
056	Pago Pago	USA Trust	14-17S	170-41W	1948-2003
029	Kapingamarangi	Fd St Micronesia	01-06N	154-47E	1978-2001
004	Nauru-B	Rep. of Nauru	00-32S	166-55E	1993-2003
030	Santa Cruz	Ecuador	00-45S	090-19W	1978-2003
254	Limetree Bay	USA	17-42N	064-45W	1982-2003

Table 4. Tide Gauge vs Model Statistics (RMS of differences in cm)					
Location (TG std.dev. in cm)		**Control**	**Std GODAS**	**T/J GODAS**	**E/E GODAS**
		1993-2003*			**1996-2003***
Guam (8.80)	RMS	9.71	4.64	3.17	2.73
	COR	0.54	0.88	0.93	0.96
Majuro (7.17)	RMS	6.43	4.50	3.22	3.42
	COR	0.56	0.82	0.90	0.90
Pago Pago (7.83)	RMS	4.80	3.12	2.25	2.29
	COR	0.80	0.92	0.96	0.97
Kapingamarangi (8.28)	RMS	5.00	3.75	3.18	3.43
	COR	0.82	0.89	0.93	0.94
Nauru (9.02)	RMS	5.05	5.30	4.38	4.02
	COR	0.85	0.81	0.88	0.93
Santa Cruz (9.04)	RMS	4.39	2.73	2.10	1.97
	COR	0.88	0.96	0.97	0.98
Limetree Bay (3.79)	RMS	3.47	3.59	2.73	2.84
	COR	0.45	0.65	0.74	0.75

* Nominal record lengths. Individual records may vary due to gaps in tide gauge records.

Table 5. TAO equatorial current observations	
Location	**Dates**
147E	5/1994-12/1997; 3/1999-12/2000; 10/2002-10/2003
165E	1/1993-12/1994; 5/1995-11/2003
170W	1/1993-12/2003
140W	1/1993- 8/1995; 9/1996-12/2003
110W	1/1993- 4/1994; 6/1994-12/2003

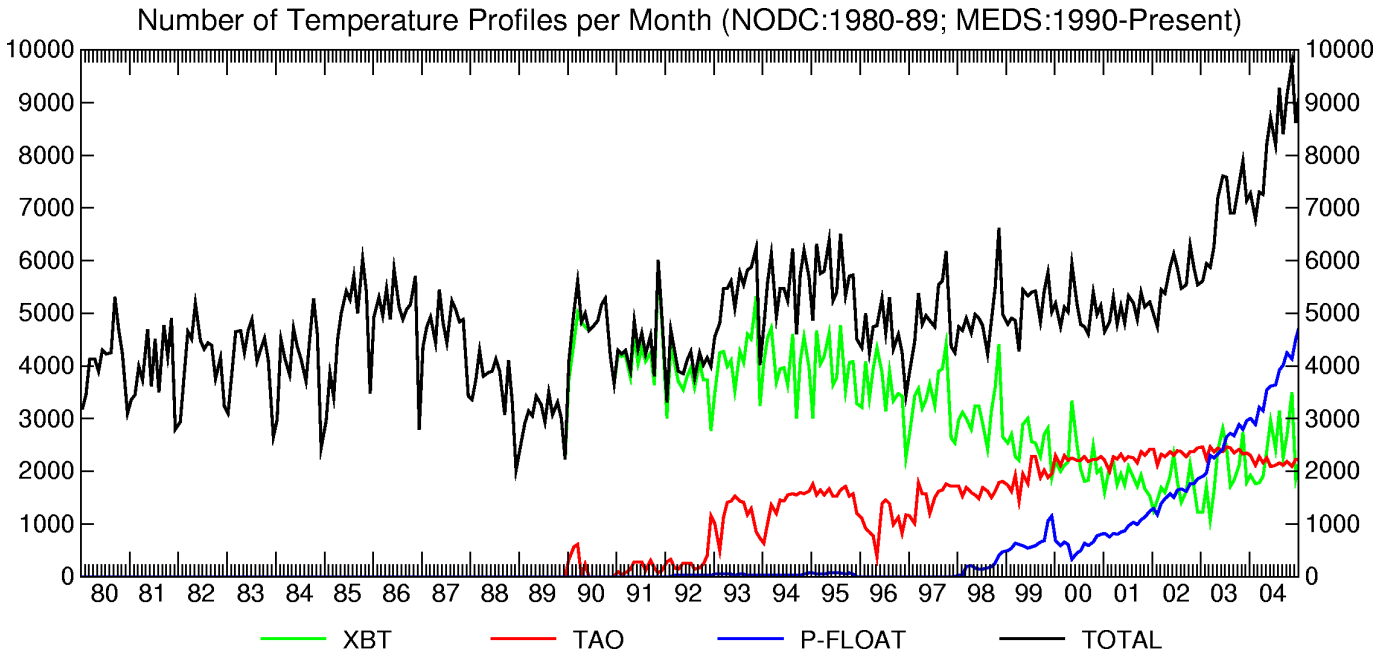

Figure 1. Monthly counts of temperature profiles used in GODAS.

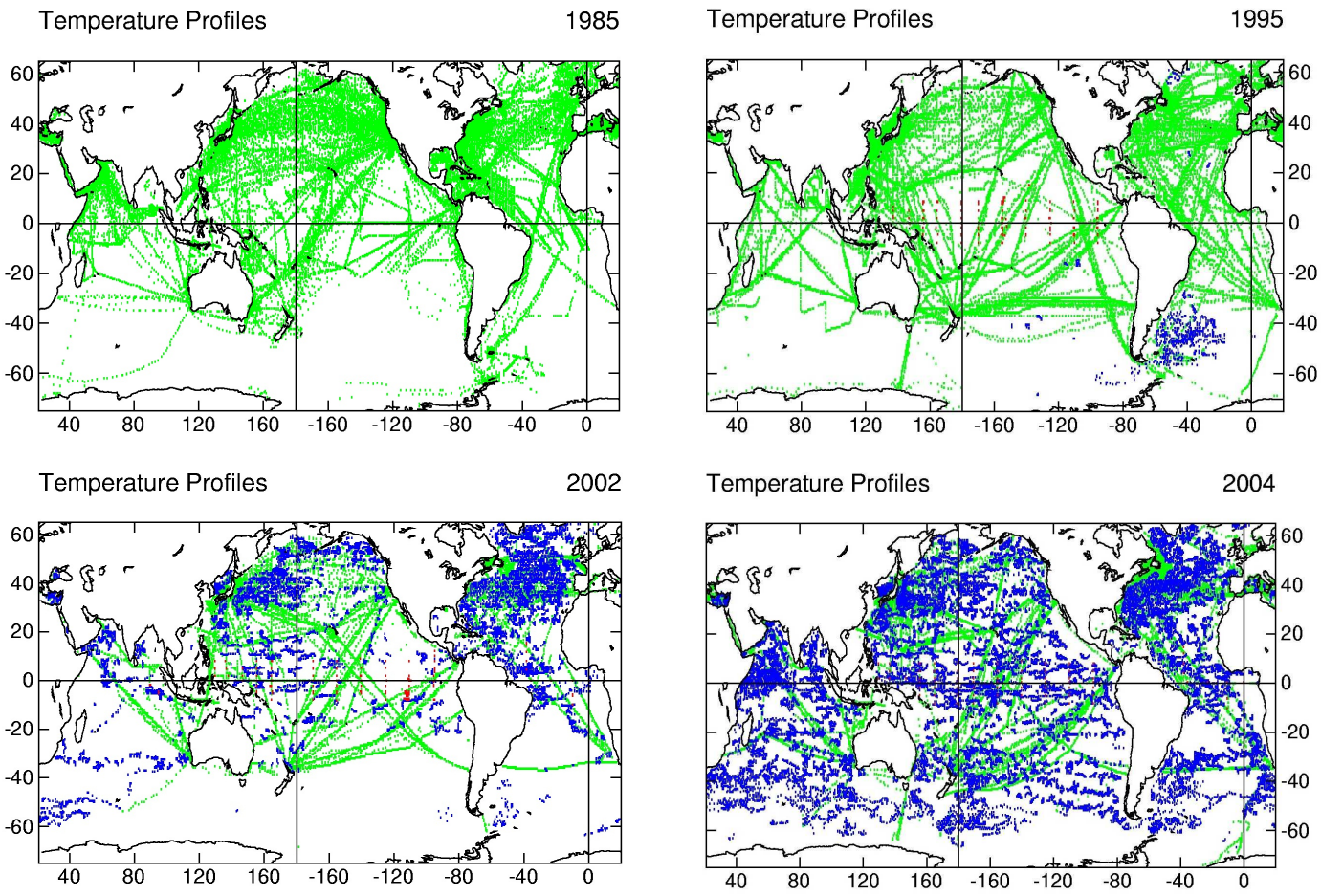

Figure 2. Annual distributions of temperature profiles. XBTs - green, Moorings - red, Argo and Argo-like floats - blue

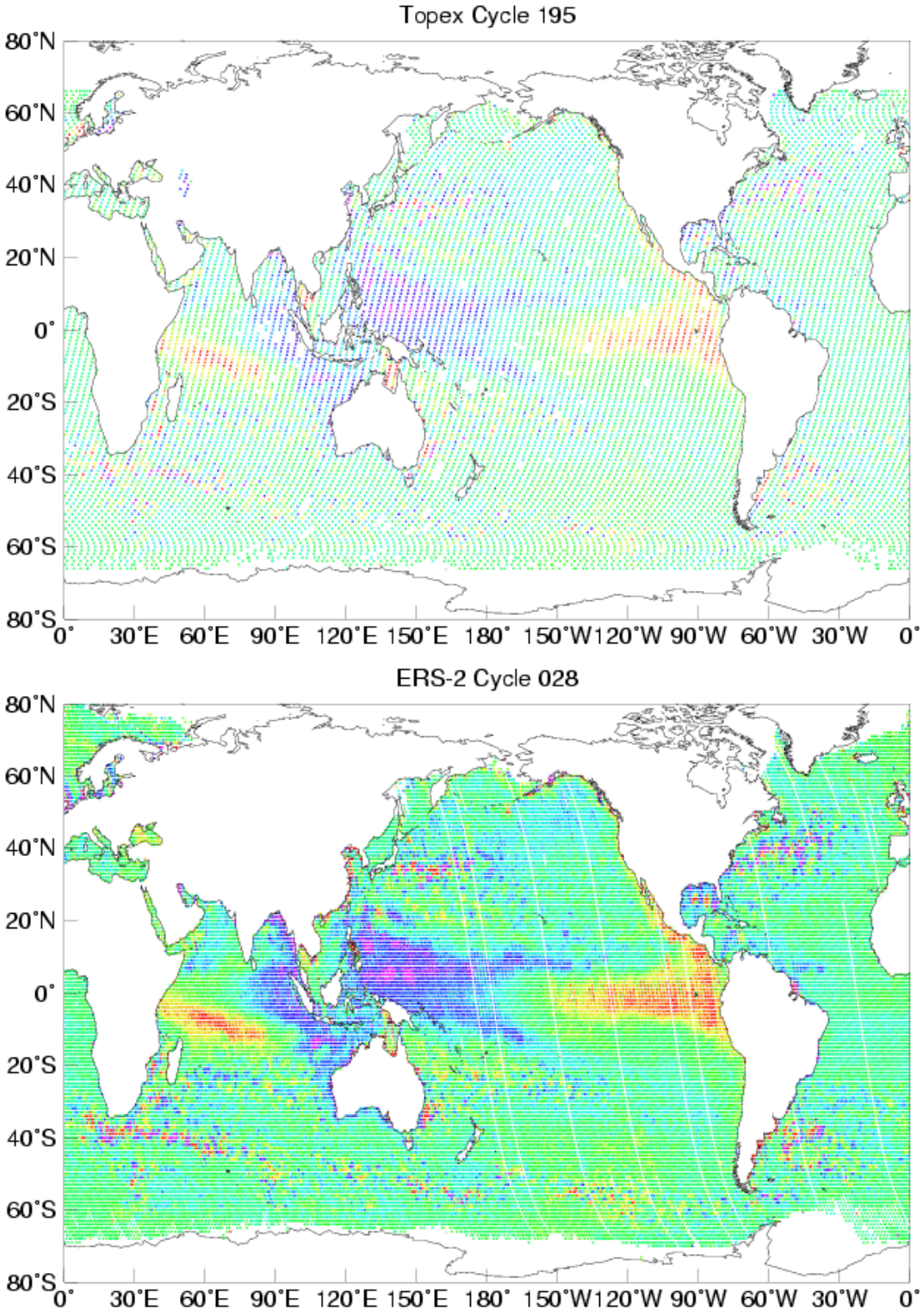

Figure 3. Examples of along-track SSH deviations. Top: a TOPEX cycle (10 days). Bottom: an ERS-2 cycle (35 days).

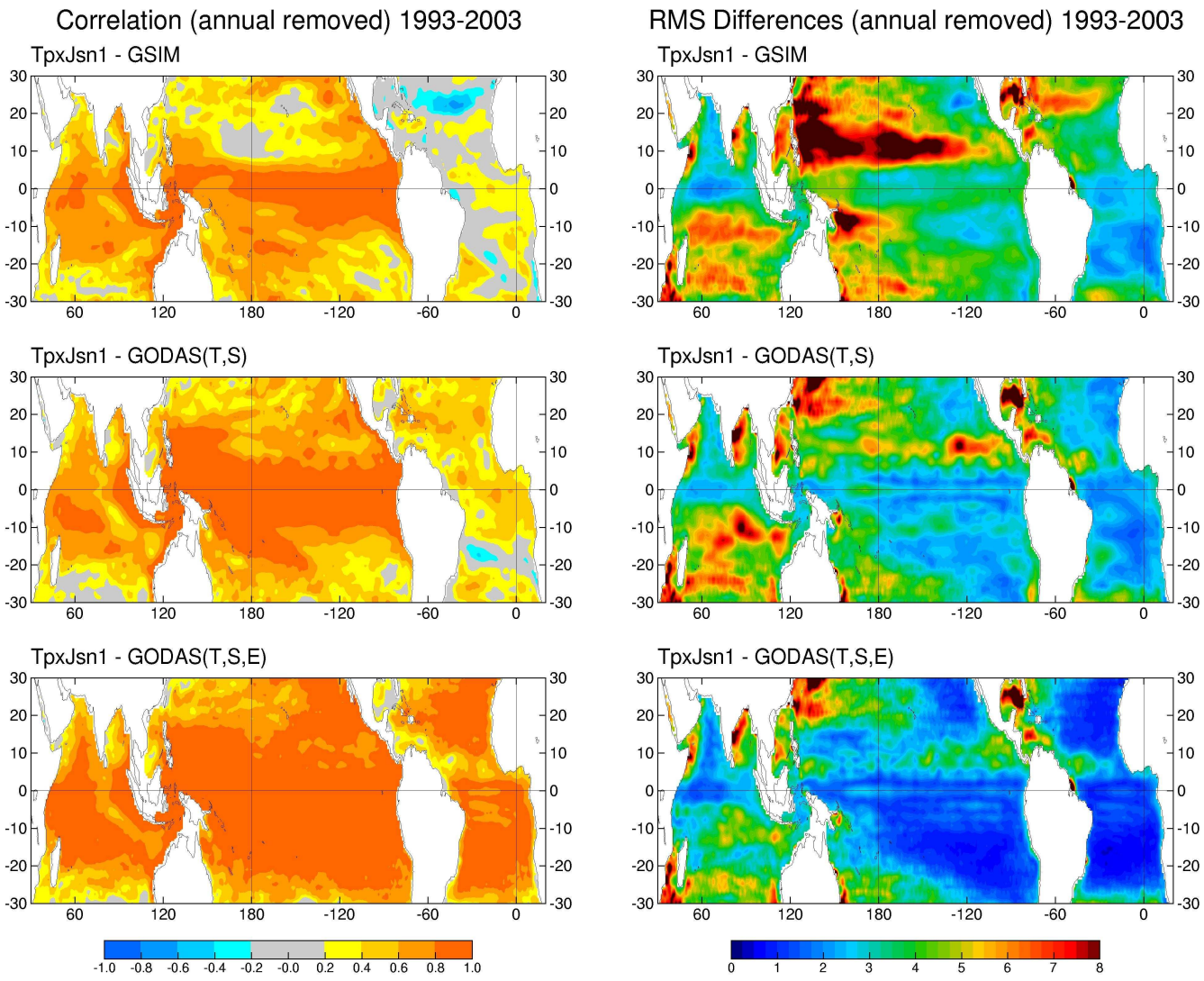

Figure 4. Correlation and RMS differences between model and TOPEX/Jason-1 SSH anomalies. Top to bottom: the control, the standard GODAS, the GODAS assimilation of TPX/Jsn-1.

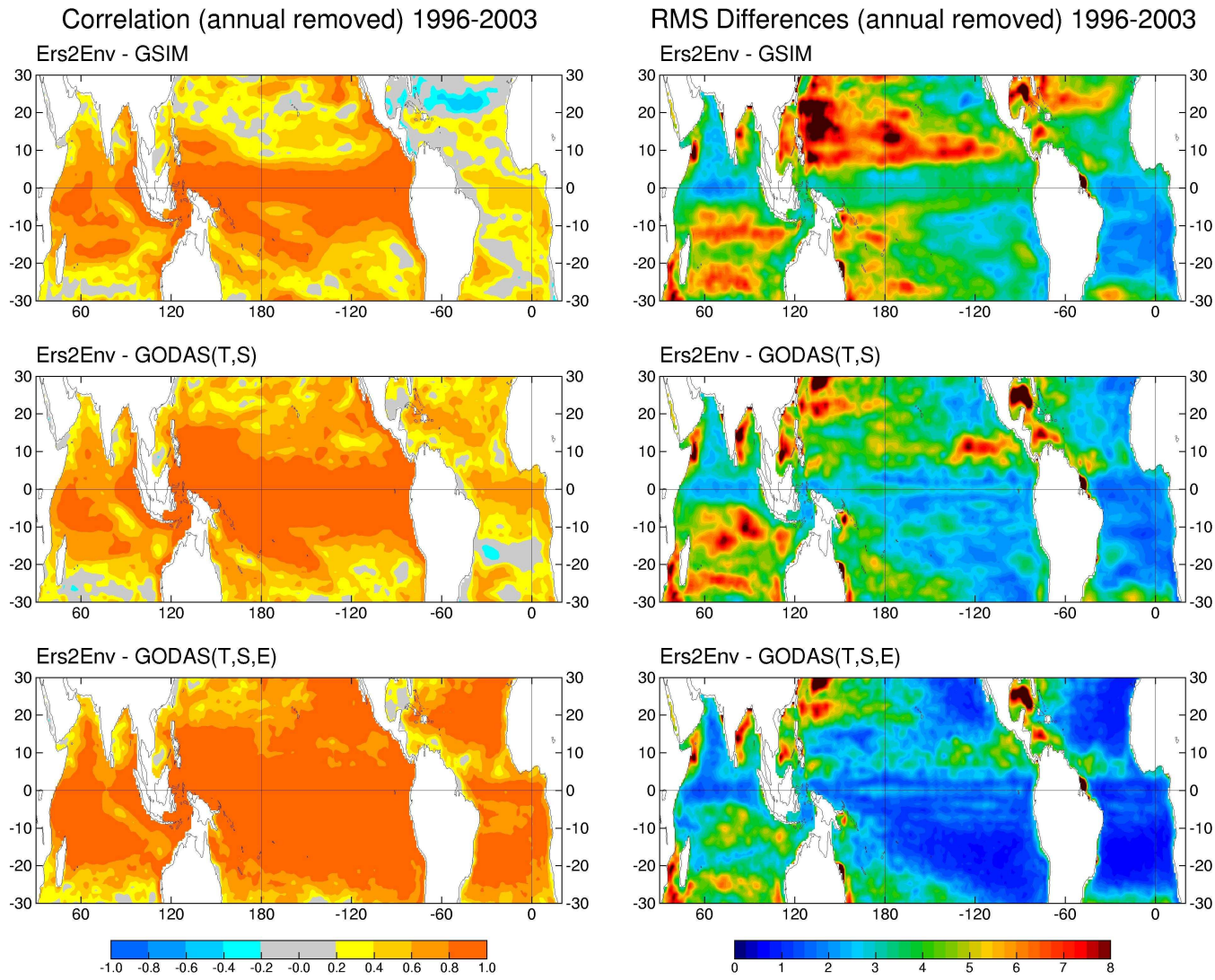

Figure 5. Correlation and RMS differences between model and ERS-2/Envisat SSH anomalies. Top to bottom: the control, the standard GODAS, the GODAS assimilation of ERS-2/Envisat.

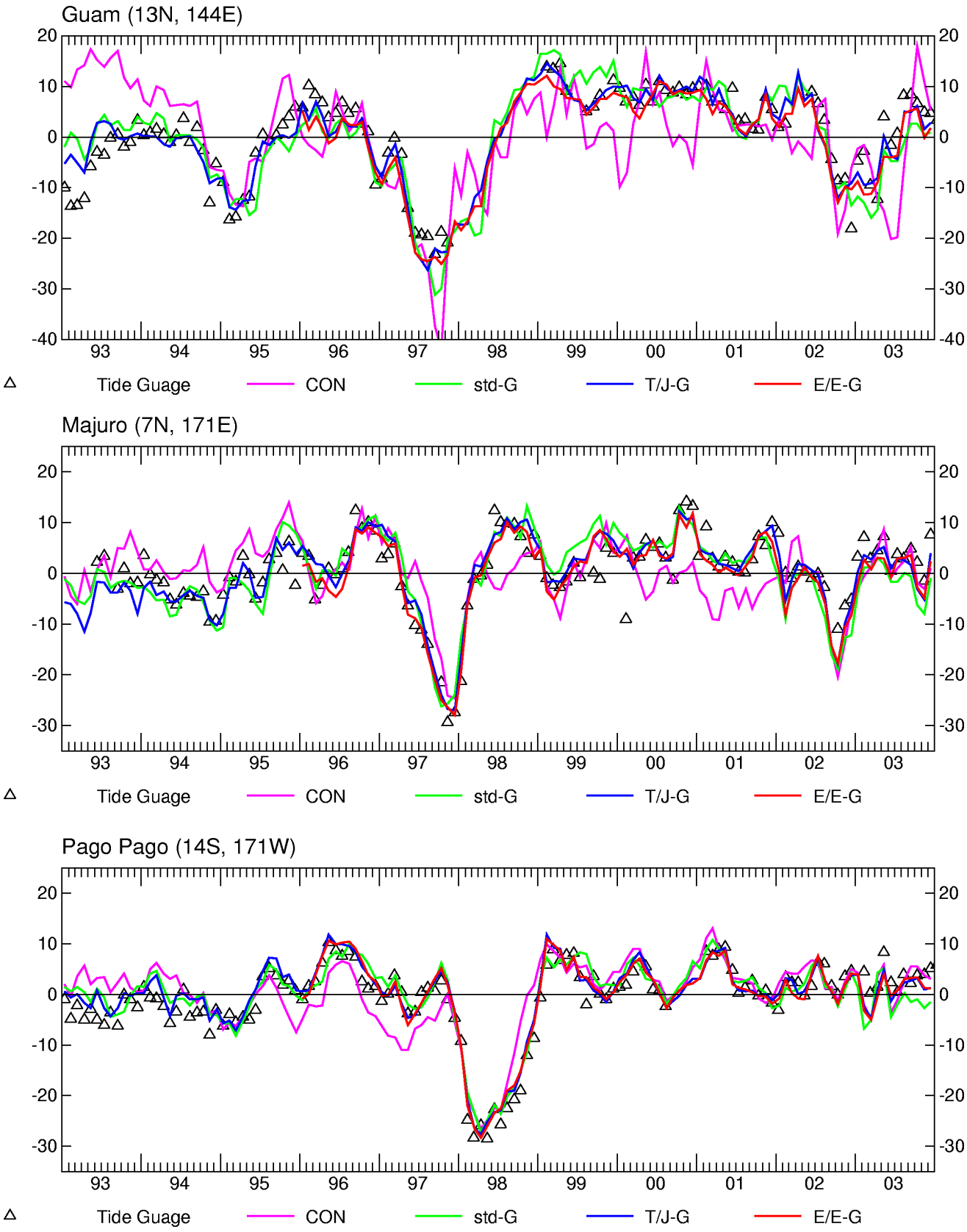

Figure 6a. Comparison of tide gauge SSH with model SSH at Guam, Majuro and Pago Pago.

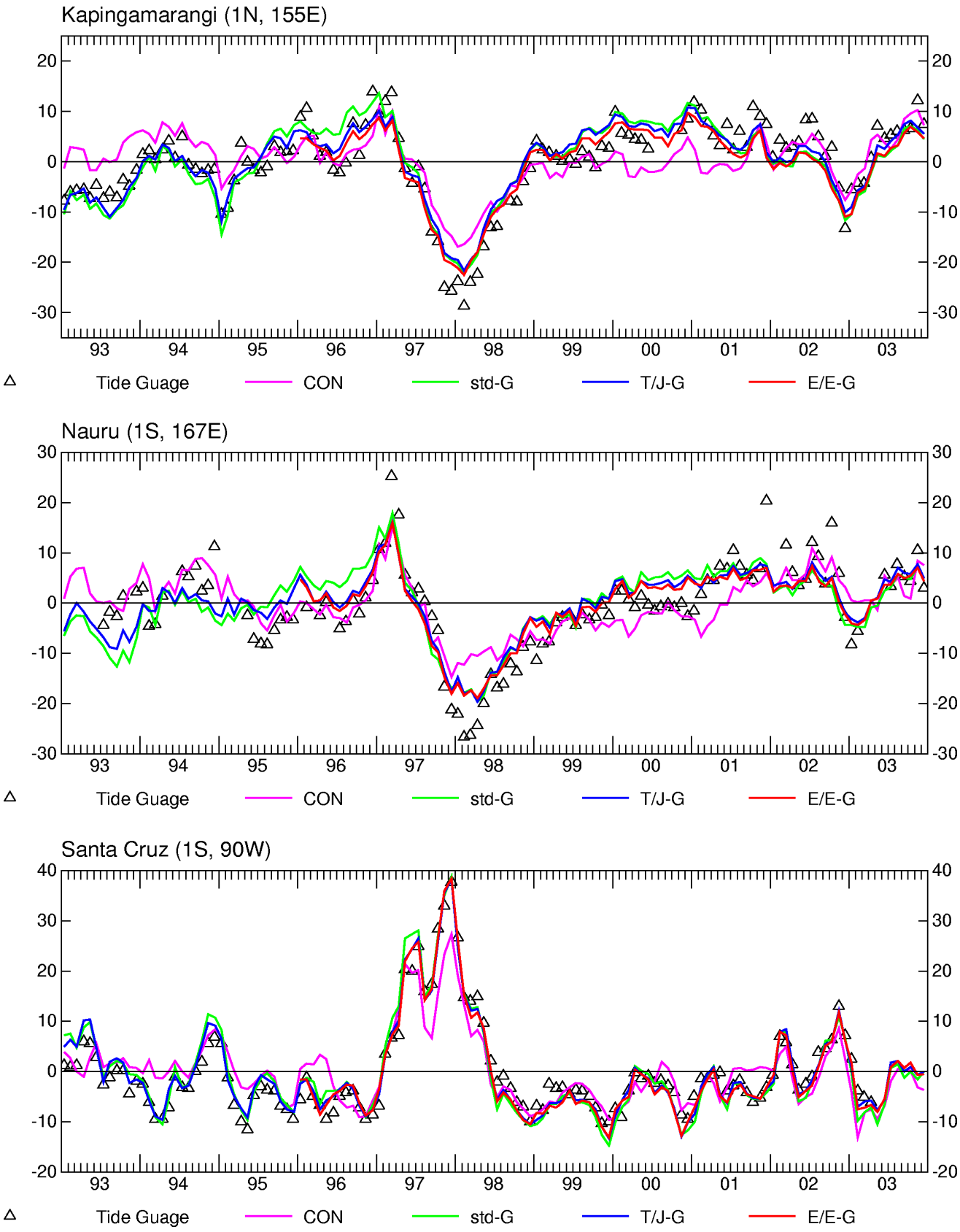

Figure 6b. Comparison of tide gauge SSH with model SSH at Kapingamarangi, Nauru and Santa Cruz.

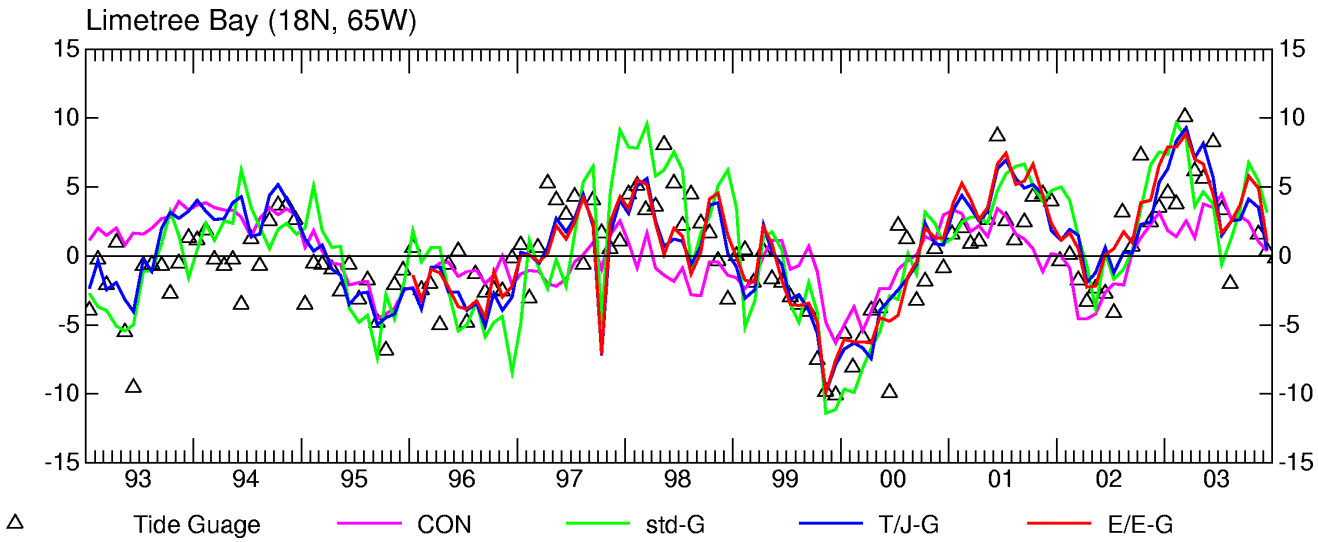

Figure 6c. Comparison of tide gauge SSH with model SSH at Limetree Bay.

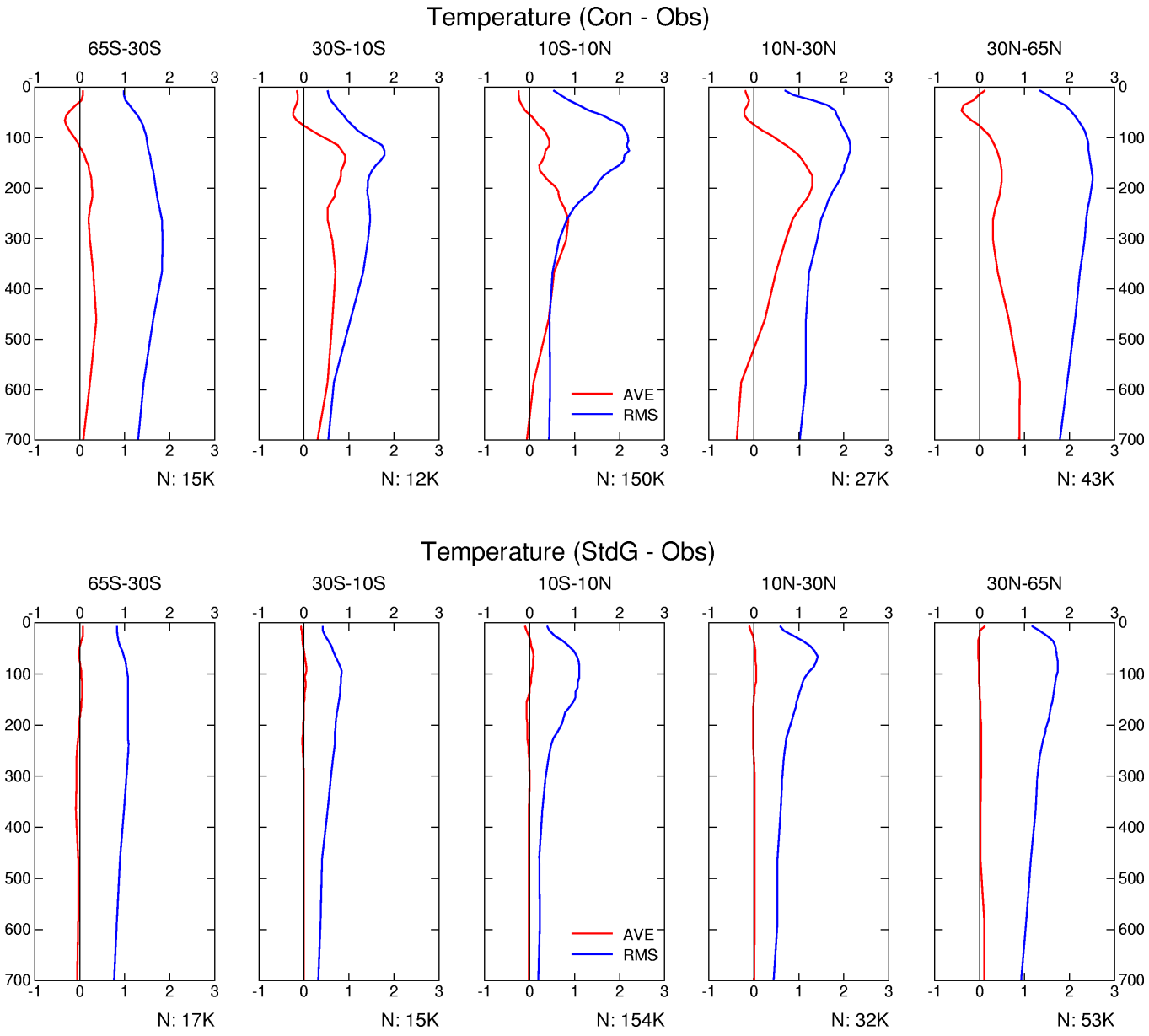

Figure 7a. Comparison of model and observed temperature profiles. Top: Control. Bottom: Std GODAS.

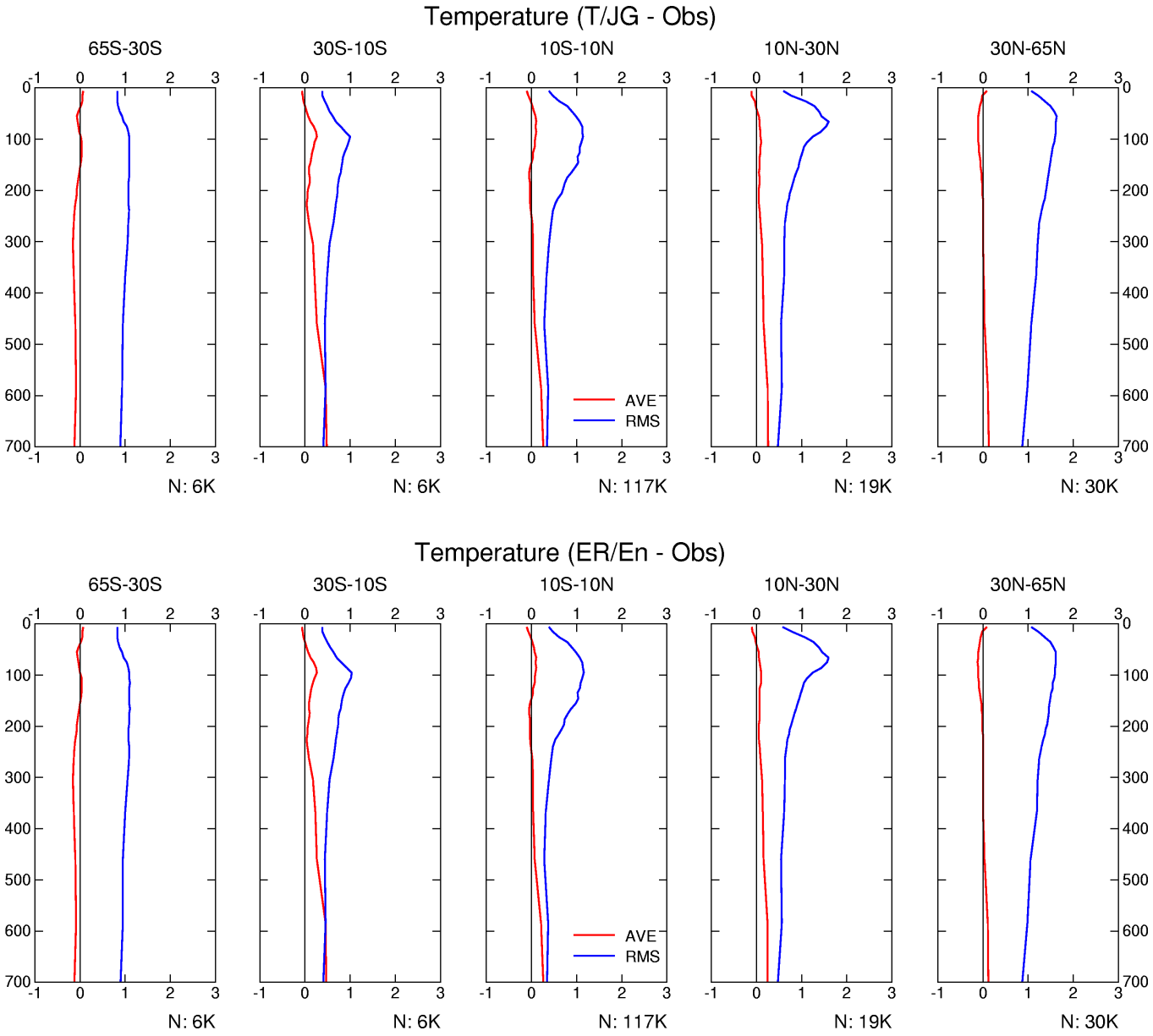

Figure 7b. Comparison of model and observed temperature profiles. Top: TPX/Jsn GODAS. Bottom: ERS/Env GODAS.

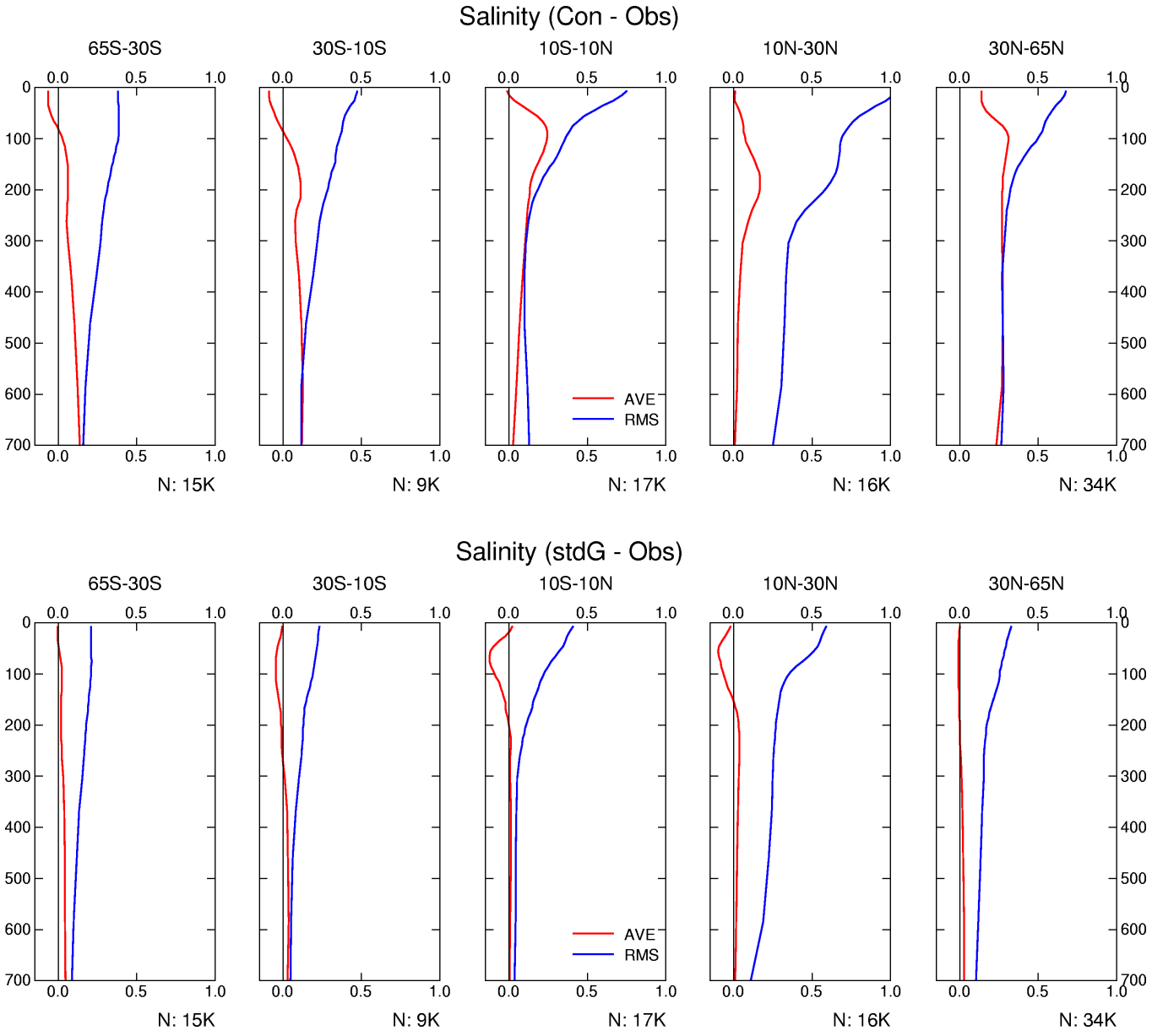

Figure 8a. Comparison of model and observed salinity profiles. Top: Control. Bottom: Std GODAS.

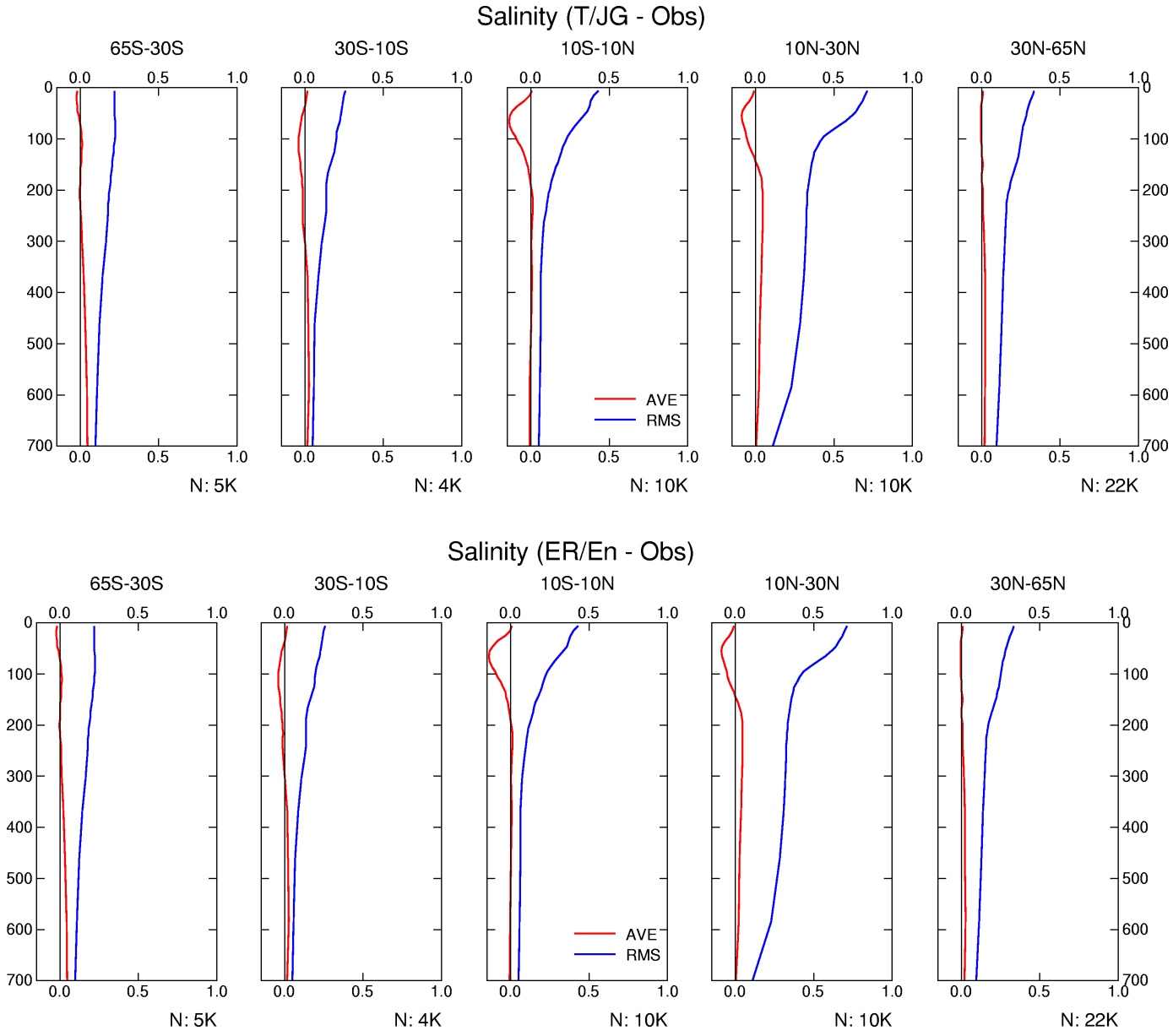

Figure 8b. Comparison of model and observed salinity profiles. Top: TPX/Jsn GODAS. Bottom: ERS/En GODAS.

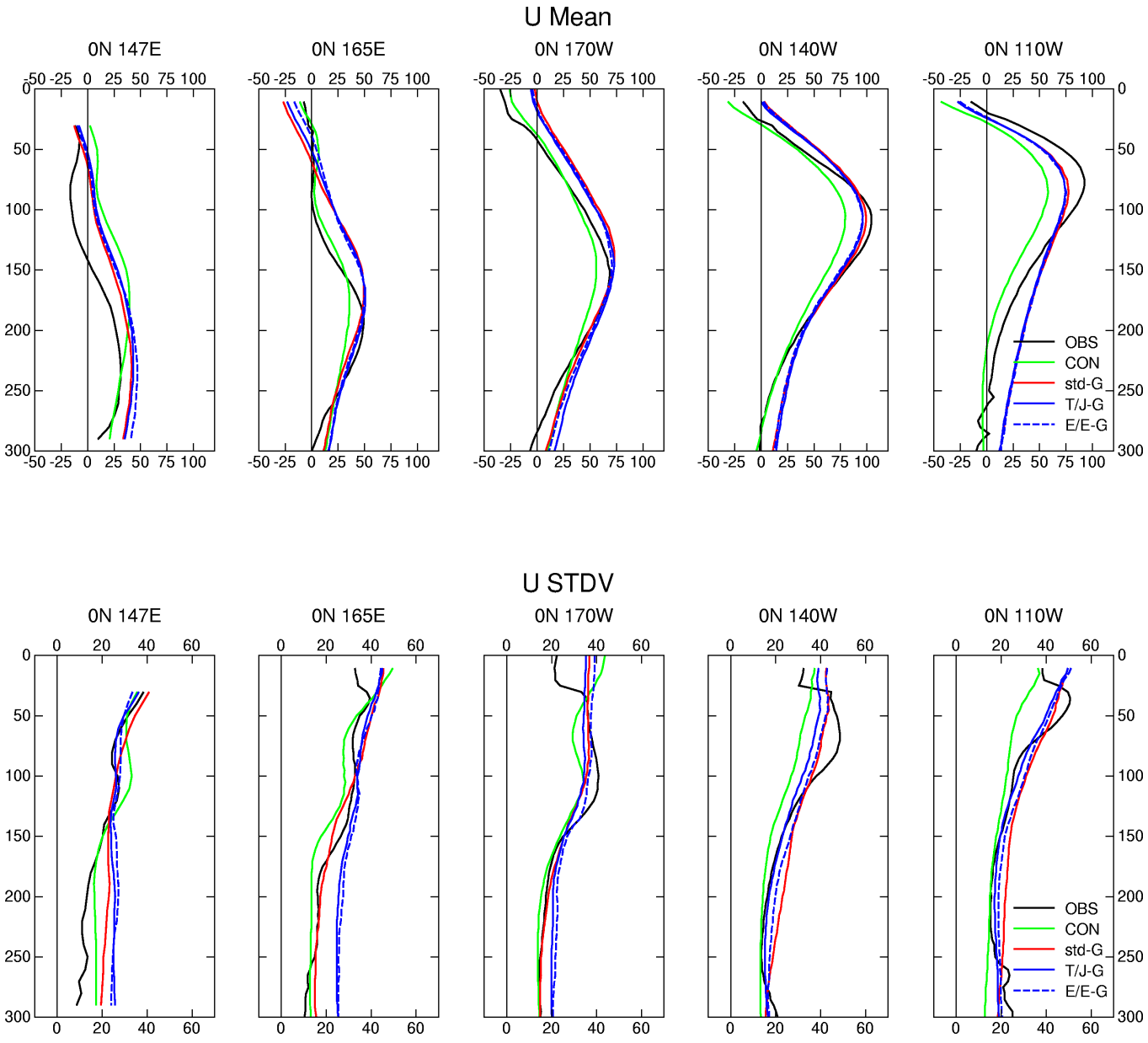

Figure 9. Comparison of model and observed equatorial zonal velocity profiles. Top: Mean. Bottom: St. Dev.